

Synthesis of nanoparticles in microheterogeneous media.

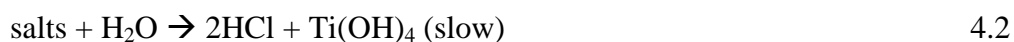
Microemulsions, micellar solutions, vesicles etc. are examples of microheterogeneous media. Apparently these solutions look homogeneous but microscopically they are highly structured and microheterogeneous having very different properties in different domains. Usually these domains are oil and water and their identity is regulated by appropriate use of surfactants. The nanosize of the structured domain has been explored by scientists to synthesize particles that because of the nanosize of domains are restricted to nanosizes. The most common vehicle for the synthesis of nanoparticles in microheterogeneous media is the microemulsion.

A microemulsion can be defined as a thermodynamically stable, optically isotropic solution of two immiscible liquids (i.e. water and oil) consisting of microdomains of one or both liquids stabilized by an interfacial film of surfactant. In water-in-oil microemulsions, the aqueous phase is dispersed as micro droplets (typically 10-25 nm in size) surrounded by a mono layer of surfactant molecules in the continuous hydrocarbon phase. The aqueous cores of the microemulsion, containing soluble metal salts, are used as micro reactors for the synthesis of nanoparticles. If two reactants A and B are dissolved in the aqueous core of two identical W/O microemulsions, upon mixing they form precipitate, AB. Due to the dynamic nature of the micro droplets, the exchange mechanism involves continuous coalescence and fusion of the droplets upon collision and subsequent disintegration in the microemulsion solution. The growth of these particles in microemulsions, is suggested to involve inter droplet exchange and nuclei aggregation.

4.1 Synthesis of Titania in Microemulsions

Titanium tetrachloride was the titania precursor used in this study. It is known that by interaction with water it gets hydrolyzed at low temperatures with the formation of volatile $\text{Ti}(\text{OH})_2\text{Cl}_2$ as an intermediate as suggested by Gruy and Pijolat (1992). Rigo et al.(1998) studied the kinetics of TiCl_4 hydrolysis they found that the reaction is split in two steps, an almost instantaneous partial hydrolysis that produces 2 mol of HCl per mol of TiCl_4 together with a salt, generally oxychloride and

hydroxyl chloride ($\text{Ti}(\text{OH})_2\text{Cl}_2$) intermediates are formed in the first partial hydrolysis step and this in a moist environment eventually hydrolyses to HCl. While the first step is very fast the salt hydrolysis was much slower, its kinetics being controlled by diffusion. These reactions can be represented as:



Even though the process is complex, a complete hydrolysis should obey the following scheme:



In the microemulsion method two similar microemulsions with cyclohexane as the oil phase but with different cores one containing TiCl_4 solution (microemulsion I) and the other containing ammonia solution (microemulsion II) were prepared and mixed as detailed in Section 3.3.1. Hydrolysis of TiCl_4 begins on mixing the two microemulsions both hydrolysis and polycondensation leading to precipitation and particle formation start immediately after the addition of titanium tetrachloride and they go on for a time that depends on the nature of the content of each microemulsion. A rough estimate of the condensation time may be obtained by visual inspection of the gelation of the solutions. This gelation time is different for different microemulsion systems. Gelation is followed by a process of evaporation of the volatile components, cooling and shrinkage of the solution, eventually precipitation occurs. Some general observations are as follows:

- i. The microemulsions I and II are both colorless after all the components are added as is characteristic of Microemulsions.
- ii. After the mixing of microemulsion II into microemulsion I, the final solution was slight white colored. This is attributed to the precipitation of titanium hydroxide.
- iii. When equal quantity of microemulsions I and II mixed immediate appearance of precipitate did not occur. This is due to the fact that the pH of mixture was low that is not favorable for immediate precipitation.
- iv. When the microemulsion II was in excess than that of microemulsion I, pH of the solution increased with addition of microemulsion II and precipitation

could be observed clearly. This is due to the presence of ammonium hydroxide in aqueous phase of microemulsion II which acts as the precipitating agent and increase in its quantity increases pH and the formation of precipitate.

- v. When subjected to stirring, the gelation time observed was different for microemulsions with different concentrations of aqueous phase. This also depended on the rate of stirring.
- vi. During stirring on a magnetic stirrer, after almost 2hrs of continuous stirring, cooling occurred first followed by the increase in viscosity of the solution. This was noted as the gelation time. On further stirring, the gel began to turn into white precipitate.

The present W/O microemulsion system, cyclohexane – Triton X-100- n-hexanol became gel within few hours after the addition of titanium tetrachloride. Usually, gelation is faster in systems containing Triton X-100 compared to that of with SDS or AOT. Triton X-100 is nonionic surfactant that forms non-spherical micelles in cyclohexane, both dry and swollen. When a titania precursor like an alkoxide added, the hydrolysis is carried out in a competitive way where water is disputed by both alkoxide and the surfactant molecule. Thus the hydrolysis rate is highly controlled and gelling is favored, since the reaction between two hydroxyl groups of the hydrolyzed species is the equally probable for further hydrolysis. This is the reason that Triton-based samples gels fast.

In post processing the precipitate obtained was washed and separated in a centrifuge at 5000 rpm, the separation was not proper that the mother liquor was still somewhat white colored which indicated that a certain amount of precipitate was still in it. Same was observed when high speed centrifuge operating at 10000 rpm was used. This indicates that the particle size was so small that its settling velocity is not attained which the existing centrifuge. Speed higher than 10000 rpm needs to be used.

The microemulsion composition was maintained constant in all the experiments and the effect of concentration of aqueous TiCl_4 solution and aqueous ammonia solutions was investigated. Initially concentrations used were 0.3 M TiCl_4 solution and 1.2 M ammonia solution. The concentration of TiCl_4 and ammonia solution was then varied to observe the variation in gelation time and the morphology of particles. The concentration of TiCl_4 solution was increased to 0.5 M and the

concentration of ammonia solutions was changed to 1 M and 1.5 M. The volumetric composition of these combinations is given in Table 4.1

Table 4.1 Composition of microemulsion and gelling time

Sample Composition			0.3M TiCl ₄ - 1.2 M NH ₄ OH		0.5M TiCl ₄ - 1.5 M NH ₄ OH		0.3M TiCl ₄ - 1.0 M NH ₄ OH	
Microemulsion		Wt	Volume %		Volume %		Volume %	
I	II	%	I	II	I	II	I	II
Aqueous TiCl ₄ Solution	Aqueous Ammonia Solution	8	6.138	6.342	5.968	6.376	5.968	6.357
Triton X- 100	Triton X- 100	19	15.098	15.065	15.124	15.059	15.124	15.062
n-hexanol	n-hexanol	15	15.59	15.561	15.622	15.55	15.622	15.557
cyclohexane	cyclohexane	58	63.175	63.038	63.286	63.01	63.286	63.024
Gelling Time			~4 hrs 12 Mins		~2 hrs 54 Min		~4 hrs 40 Min	

Hydrolysis and polycondensation start immediately after the addition of titanium tetrachloride and they go on for a time that depends on the nature of the content, i.e. the content of each solution. A rough estimate of the condensation time may be obtained by visual inspection of the gelation of the solutions. This gelation time is different for different microemulsion systems. Gelation is followed by a process of evaporation of the volatile components, cooling and shrinkage of the solution. Eventually precipitation occurs. The present W/O microemulsion system, cyclohexane – Triton X-100- n-hexanol became gels within few hours after the addition of titanium tetrachloride as reported in the Table 4.1.

The precipitates obtained are washed with methanol-chloroform mixture and were dispersed in various solvents like n-propanol and acetone. A drop of the dispersed solution was taken on a microscope glass slide and heated to 450⁰C for 2h. The heated glass slide was cooled and examined using a scanning electron microscope to observe the particle size and morphology. Material characterization was done using XRD and FTIR, thermal characterization was done using TGA.

4.2 Material Characterization

Precipitates from a number of experimental runs performed under identical conditions with precursor concentration ($\text{TiCl}_4 = 0.3 \text{ M}$ and $\text{NH}_4\text{OH} = 1.2 \text{ M}$) were collected and subjected to calcinations at temperatures ranging from 500°C to 700°C and time ranging from 1 hr to 2 hr. Pure rutile phase was obtained as revealed by XRD analysis when Calcination temperature was 680°C and duration was 2 hr. Crystallite size was found to be 47.7 nm with cell parameters $a = 4.592$ and $c = 2.958$, in general the shape of the crystal was tetragonal. Reduction of calcinations temperature led to the formation of anatase phase which had a lower crystallite size (14.5 nm). Increase in crystallite size is attributed to phase transformation, soaking and thermal effects. Fig 4.1 presents the relevant XRD profile of the particles.

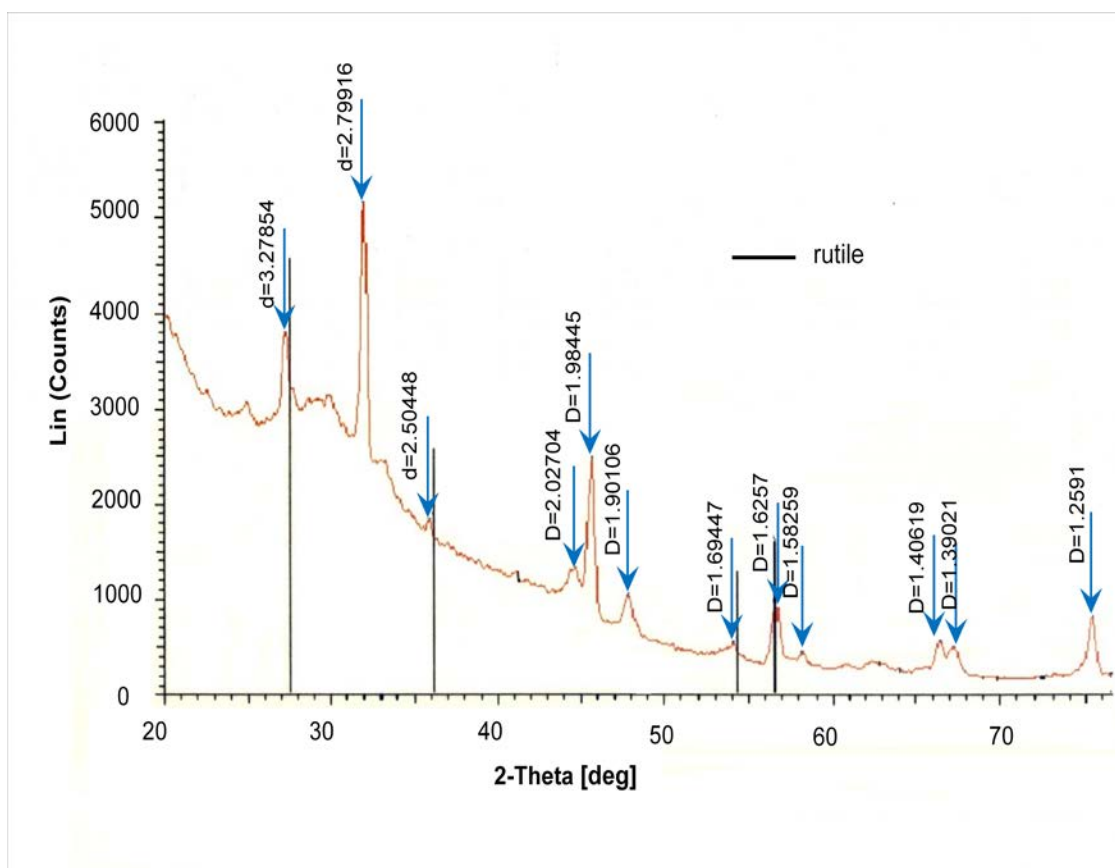


Fig 4.1 XRD pattern of TiO_2 sample calcined at 680°C containing 100 % rutile

Figures 4.2 show the DTA and TGA results of the precipitate sample which was heated at the rate of $20^\circ\text{C}/\text{min}$ up to 800°C starting from 40°C in oxygen atmosphere. Three weight loss regions were observed on the TGA curve.

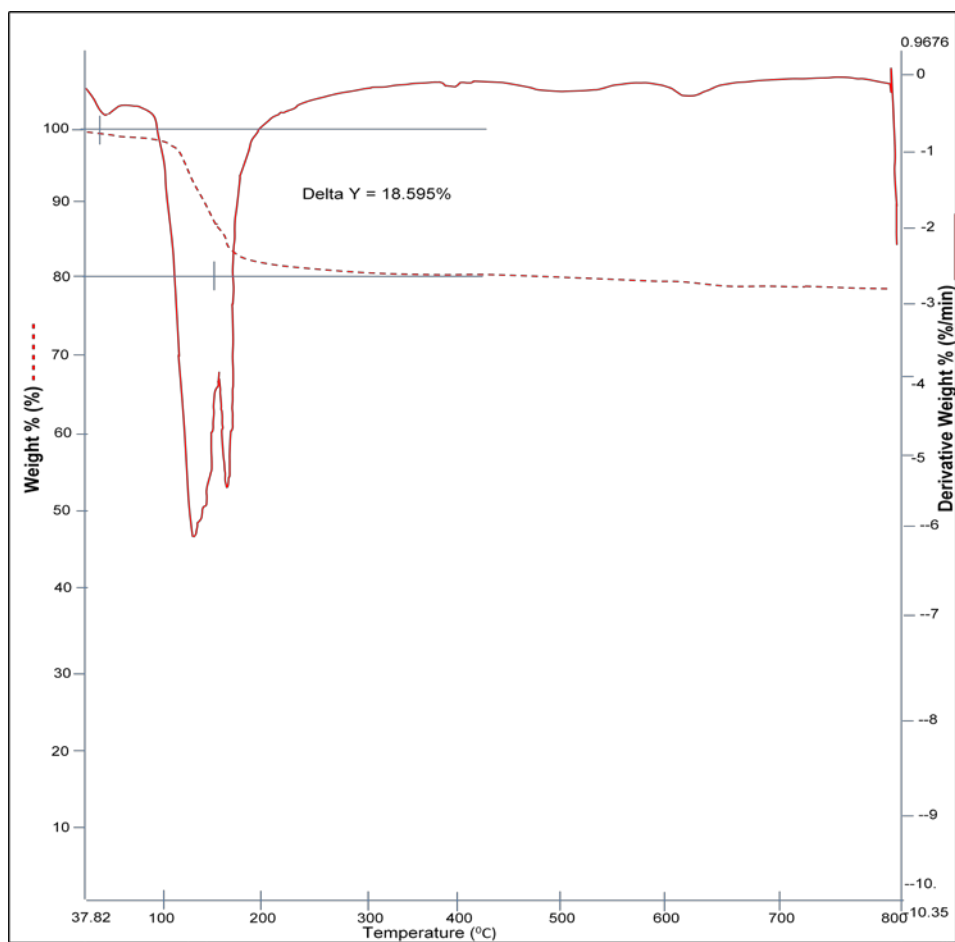


Fig 4.2 DT-TGA of precipitate samples from microemulsion synthesis of Titania

Initial weight loss in the 40 – 200^o C, was primarily due to the removal of physically absorbed water i.e, the removing of –OH group. The weight loss at 200^o C-400^o C range was mainly caused by the removal of acidic HCl. There was no apparent weight loss after 400^o C for the samples. The total weight loss for the sample prepare was 20.97 %.

The DT analysis of the product indicates prominent endotherms below 180^o C which can be mainly due to the free adsorbed water. However, there is only one sharp endotherm for the sample There is a broad exothermic shoulder from 200-380^o C which corresponds to the decomposition of residual –OH groups and the condensation of non-bonded oxygen. The process continues with the exothermic shoulder which indicates the increase in crystallization of anatase phase. At round 580^o C, the product completely transforms into anatase. After 620^o C, there is a constant exotherm which indicates the appearance of rutile phase and there after no significant thermal effects are observed.

The precipitates synthesized using precursor concentration of 0.5 M TiCl_4 and 1.5 M NaOH subjected to calcinations at 580°C did not result in a pure phase but a mixed phase of Rutile and anatase as revealed by the XRD pattern shown in Fig. 4.3

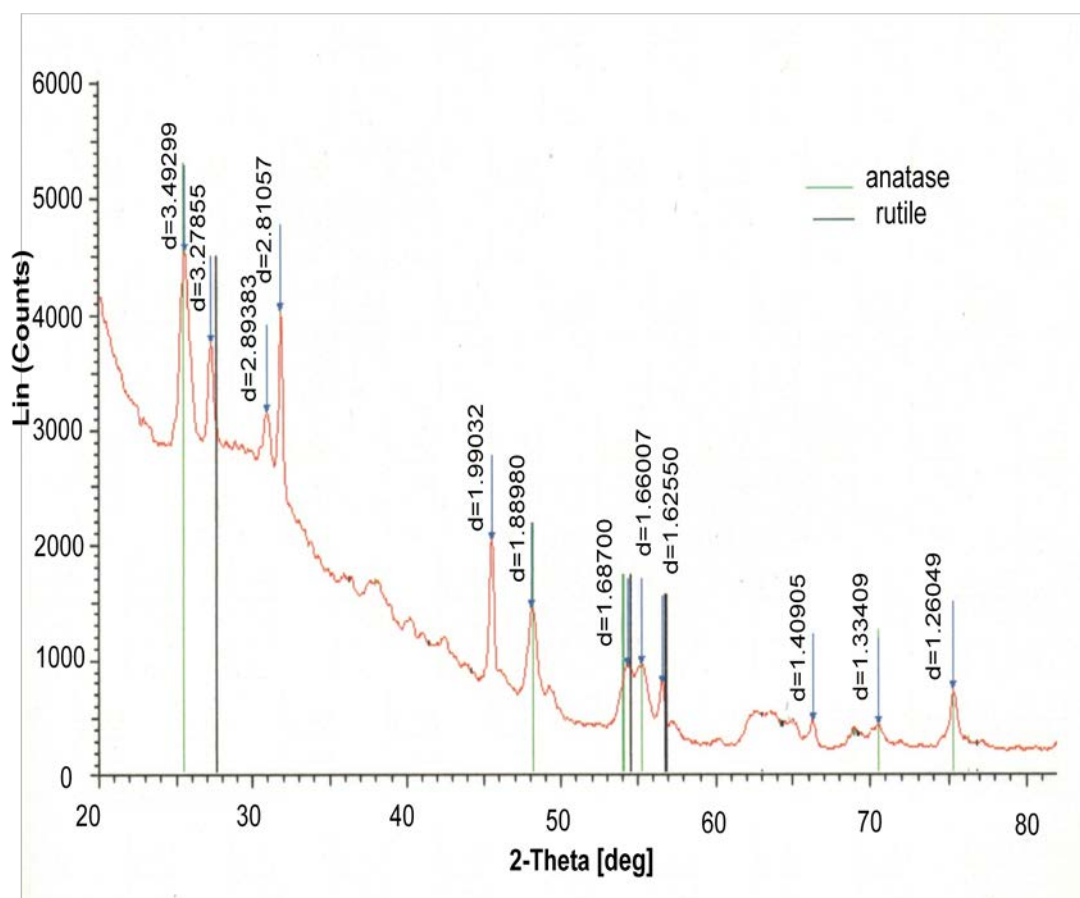


Fig 4.3 XRD pattern of TiO_2 sample calcined at 580°C containing 66.8% anatase and 33.2 % rutile

4.3 Morphological analysis

The samples prepared with different concentration of precursors showed different morphologies Figures 4.4 (a) and (b) show the SEM images of samples dispersed in acetone and propanol respectively. From these images it can be observed that agglomeration of the particles was more in case acetone as the dispersed medium (Fig 4.4 (a)). The particle size was estimated to be around 100 nm.

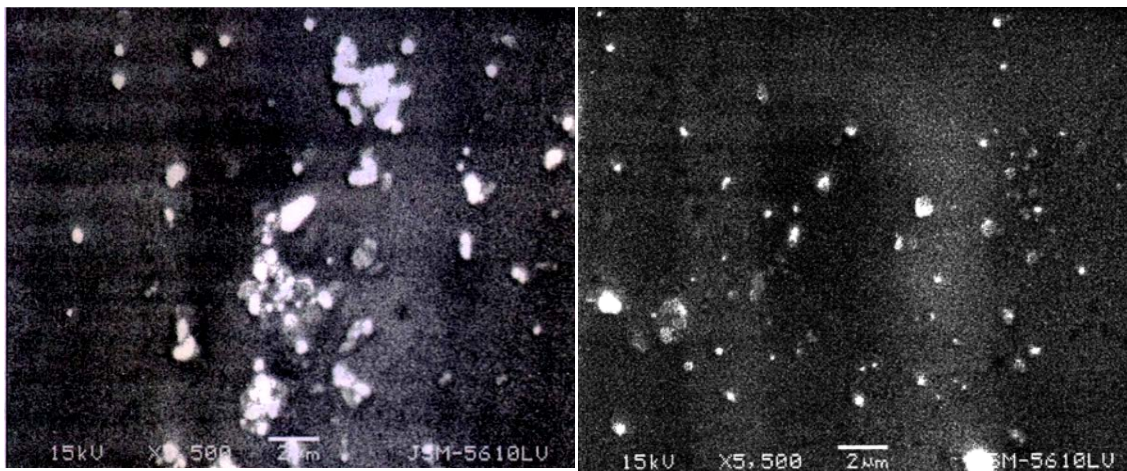


Fig 4.4 (a) SEM image of as prepared sample Dispersed in acetone

Fig 4.4 (b) SEM image of as prepared sample Dispersed in propanol

Figure 4.5(a) and (b) show the SEM pictures of TiO_2 particles obtained by varying the concentrations of aqueous solutions in the microemulsions. It can be observed that by changing the concentration of the aqueous solutions the morphology obtained was different. By increasing the concentration of TiCl_4 solution, particle agglomeration was more. Same was observed for an increase in ammonia concentration. The particle size obtained in latter is more than that obtained in the former.

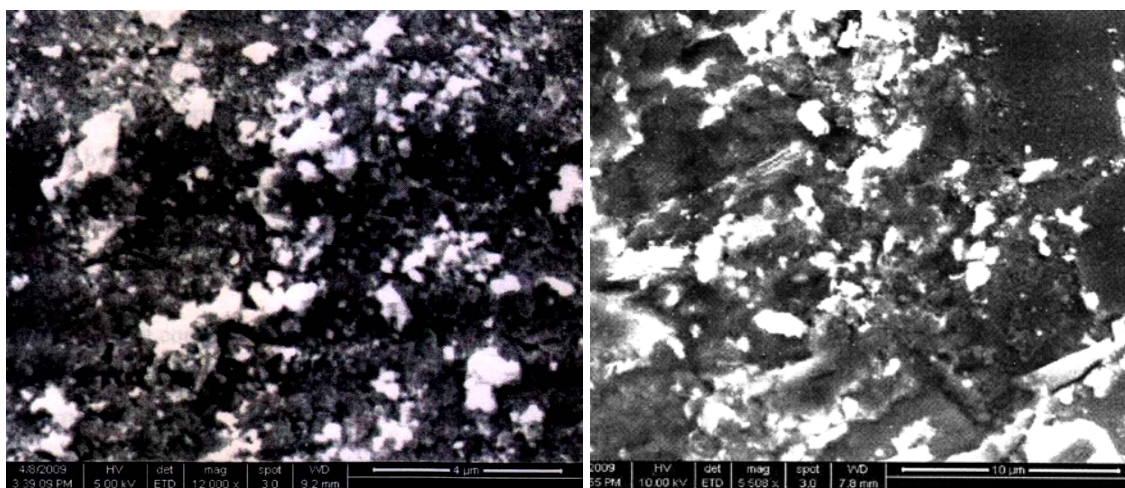


Fig. 4.5(a) SEM image of samples with 0.5 M TiCl_4 and 1.5 M NH_4OH

Fig. 4.5(b) SEM image of samples with 0.5 M TiCl_4 and 1.0 M NH_4OH

4.4 Synthesis of Titanium dioxide by Sol-Gel route

Sol-Gel processing is one of the routes for the preparation of porous materials by their solidification from a true solution phase, and its physio-chemical principles and applications. The method is characterized by the formation of stable colloidal solutions (“sol”) in the first step, followed by anisotropic condensation of colloidal particles (micelles) producing polymeric chains with entrapped solution of condensation byproducts, resulting in the formation of a “liogel” or “hydrogel” or “monolith” when external solvents is not used. After washing out the byproducts, the solvent removal produces “xerogels” or “aerogels” depending on the drying mode, with distinct structures of the primary particles and their packing maner.

For clarity of terminology the sol-gel method should be distinguished from other routes of materials solidification from solutions, such as precipitation and deposition from precipitation, crystallization from melts, expansion of super critical solvent, supercritical antisolvent method, super molecular assembling, and others. The main peculiarity-which makes the sol-gel route unique and clearly discernible- is the formation of a clear colloidal solution due to primary condensation of dissolved molecular precursors. The second peculiarity is the merging of these colloidal particles during the subsequent gelation stage into polymeric chains by chemical bonding between local reactive groups at their surface. This prevents flocculation that is result of isotropic micelle aggregation. The porous solids (xero or aerogels) are produced in the next step-desolvation-dependng on the drying mode.

Both stages are controlled by condensation chemistry that can include, as first step, the hydrolysis of hydrated metal ions or metal alkoxide molecules (hydrolytic sol-gel processing). The condensation chemistry in this case based on olation /oxolation reactions between hydroxylated species. The hydroxylated species for further condensation can also be formed by a non-hydrolytic route; that is, by reactions between metal chlorides and alcohols with electron-donor substituents. The non-hydrolytic sol-gel processing may also proceed without intermediate formation of hydroxylated species when it is based on esterification of metal chelate complexes with free carboxylic groups and polyalcohols. Another non-hydrolytic/non hydroxylating sol-gel route relies on direct condensation reactions between metal

alcoxides and metal chlorides or acetates, with the elimination of alkylchlorides or esters.

The characteristics of sol-gel processing allow the application of different strategies for the preparation of solid catalytic materials. The gelation of colloidal solution, followed by desolvation of the obtained gel, can be applied for the preparation of three types of materials:

1. Bulk uniphasic materials, i.e, mono or multimettalic xero-or aerogels
2. Bulk multiphasic materials where molecular moieties or condensed phases are entrapped between polymeric chains of the gel matrices and/or co-gelated from a mixed colloidal solution
3. Porous uni- and multiphasic coating and nanometirc films prepared by conducting the gelation inside a thin film of colloidal solution at the surface of a supporting material (substrate).

There is quite some difference of opinion regarding the nature of the sol-gel media although micro heterogeneity does exist in the media but it is transient and does not qualify in the same sense as the microemulsion or reverse micelles (Hench and West, 1990). Never the less the sol-gel method is the dominant and consistent technique for producing nanoparticles in sizeable quantity hence this technique also was explored and titania nanoparticles were synthesised using sol-gel route using TiCl_4 as the precursor and different alcohols like i- propanol, butanol, ethanol, benzyl alcohol as solvents. The steps: colloidization, flocculation, gelation and drying by evaporation were encountered. The effect of solvents and calcinations temperature on the phase of TiO_2 obtained was investigated.

4.5 Characterization of particles

Samples were classified by number as shown in the Table. Characterization of particles was done using FT-Raman spectroscopy, FTIR, XRD and SEM.

Table 4.2 Composition of Samples and thermal condition

Sample No	Solvent and precursor	Calcinations Temperature
1	Isopropanol + TiCl_4	450 $^{\circ}\text{C}$
2	95 % Ethanol + TiCl_4	450 $^{\circ}\text{C}$
3	Butanol + TiCl_4	450 $^{\circ}\text{C}$
4	Isopropanol + TiCl_4	Calcined at 700 $^{\circ}\text{C}$
5	95 % Ethanol + TiCl_4	Calcined at >800 $^{\circ}\text{C}$

4.5.1 Fourier Transform Raman spectroscopy

Fourier Transform Raman spectroscopy (FT-Raman)-Raman spectra of purified and dried samples were recorded by using a FT- Raman Spectrometer (Model: RFS 100/S, Bruker Optik) equipped with a 750 mW Helium : Neon laser source operating at 1064 nm having laser power 350 mW and liquid nitrogen cooled germanium detector, scanning range from (+) 4000 cm^{-1} to (-) 2000 cm^{-1} and number of scans fifty.

The FT-Raman spectra of sample-1,2 and 3 with pure solid form was scanned from -800 cm^{-1} to 3500 cm^{-1} observed a strong and three medium bands at 144 cm^{-1} , 396 cm^{-1} , 516 cm^{-1} and 639 cm^{-1} respectively which is due to the presence of B_{1g} , E_g and A_{1g} modes of TiO_2 . The spectral pattern with intensity ratio indicates that there is not much difference due to presence of organic solvents such as isopropanol, 95% ethanol and butanol. As seen in Fig 4.6 to 4.8.

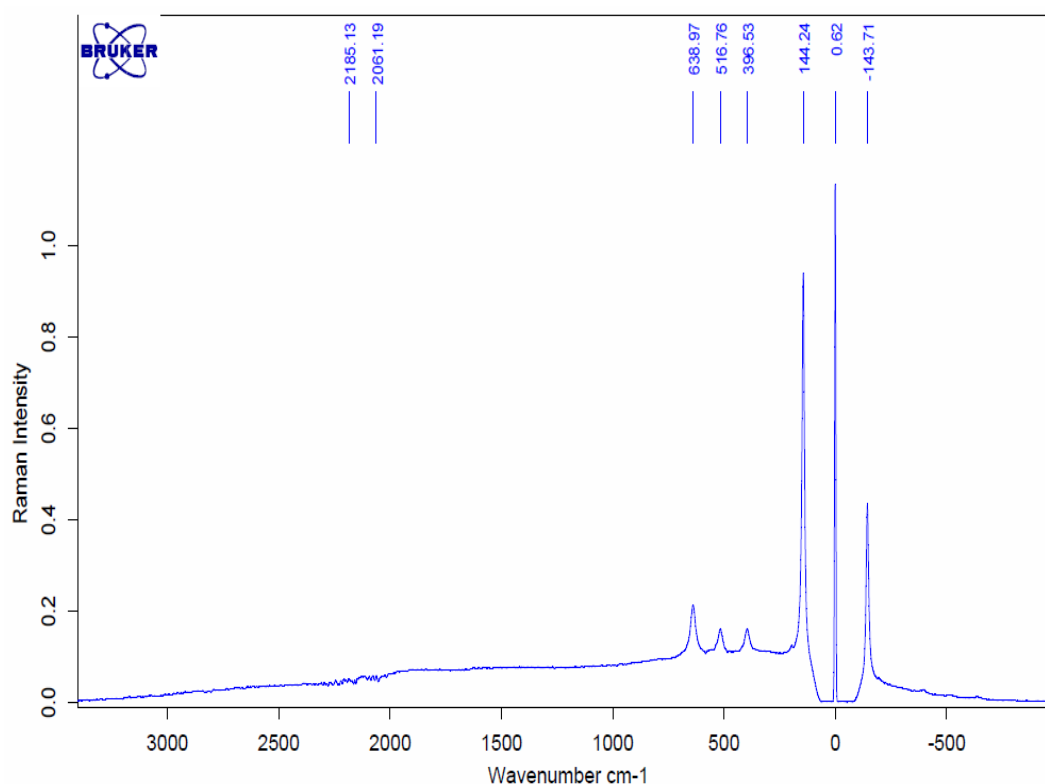


Fig 4.6 FT-Raman spectra of sample-1

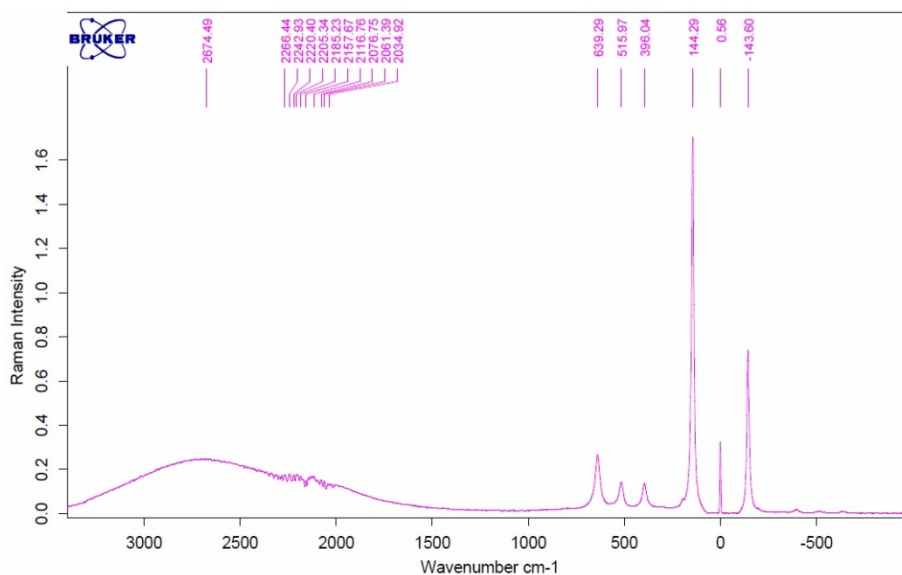


Fig 4.7 FT-Raman spectra of sample-2

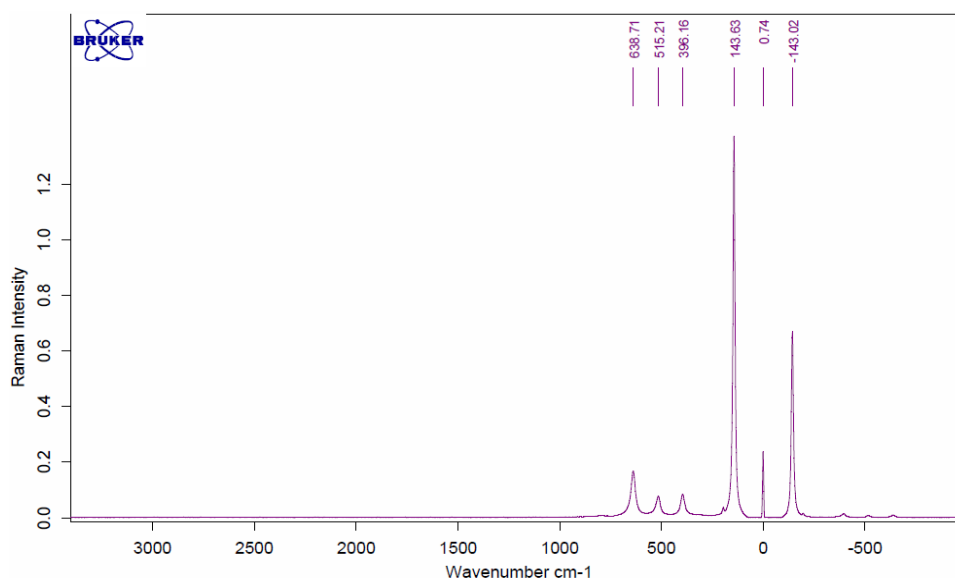


Fig 4.8 FT-Raman spectra of sample-3

For the case of sample-4, synthesized using i-propanol as solvent and calcined at 700°C. Significant new bands observed at 143.13 cm⁻¹, 447.27cm⁻¹, and 621.48cm⁻¹ Simultaneously a broadband observed at 2585 cm⁻¹ (Fig4.9). Similarly significant new bands are observed at 143.55 cm⁻¹, 236.85 cm⁻¹, 447.62cm⁻¹, and 609.76 cm⁻¹ for sample-5 synthesized using ethanol as solvent calcined at > 800⁰ C (Fig 4.10). In this case also a big broadband is observed at 2585 cm⁻¹. The new band observed at 236.85 cm⁻¹ is considered as a second-order band, which is fundamental mode of vibration due to lattice disorder induced band.

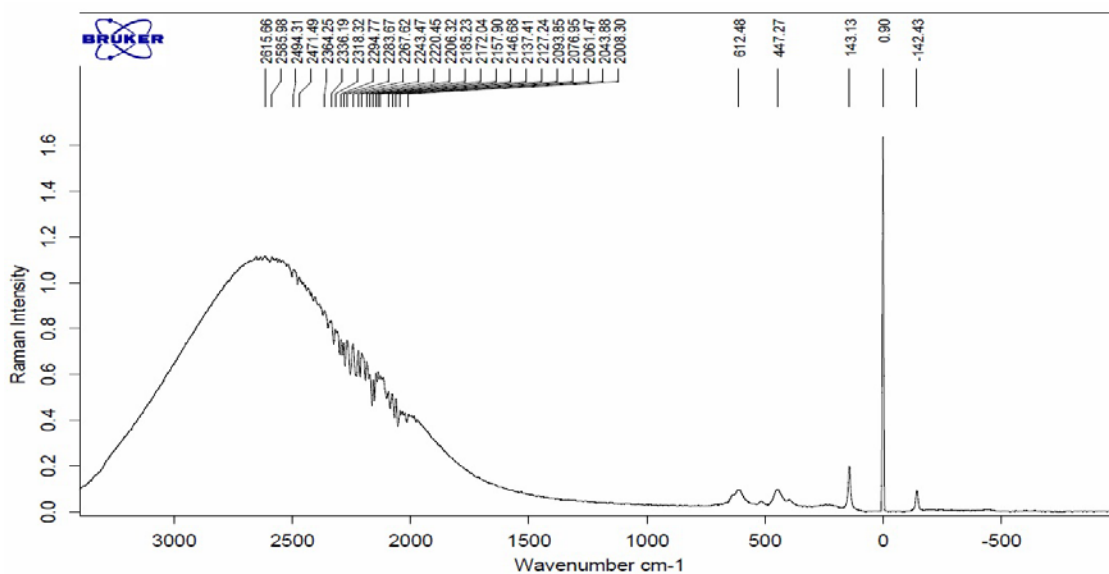


Fig 4.9 FT-Raman spectra of sample-4

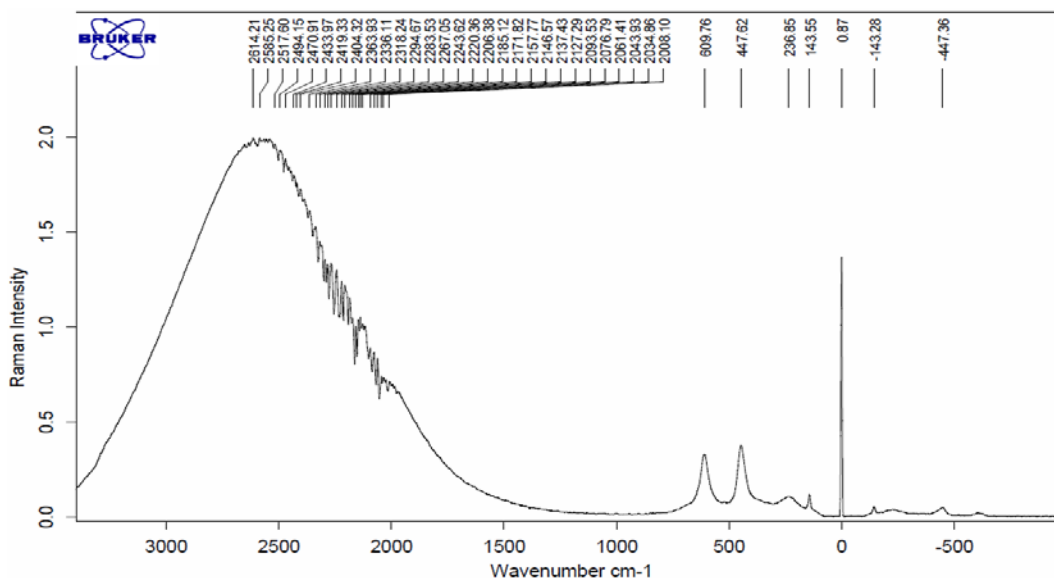


Fig 4.10 FT-Raman spectra of sample-5

4.5.2 IR Spectra

The FT-IR spectra of different samples with organic solvents (1-5) TiCl₄ over KBr pellet matrix from 400 cm⁻¹ to 4000 cm⁻¹ did not show any drastic change in spectral pattern. The sample No.4 and 5 have a significant stretching frequency (weak broad band) observed within a range at 3881-3733 cm⁻¹ which indicates the presence of -O-H bond due to the presence of intermolecular hydrogen bonding between alcoholic group with TiO₂ at high temperature.

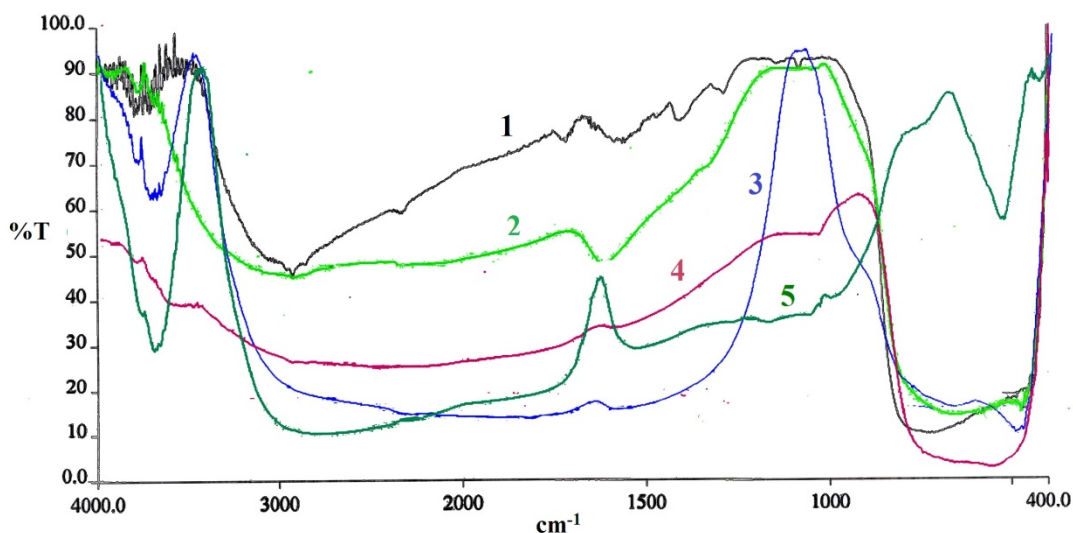


Fig-11 FT-IR spectra of different samples with organic solvents (1-5)

4.5.3 XRD Analysis

To identify the phase purity, crystallinity of the prepared sample X-Ray diffraction was done. Upon calcinations above 250 °C TiCl_4 converts to titanium oxide. In the range from 20 to 70° 2θ , the major peaks of the three crystalline polymorphs of titania namely rutile, anatase and brookite are found. Among then rutile is the most stable phase. XRD pattern of sample 1 (TiCl_4 + Isopropanol calcined at 450° C), is shown in Fig. 4.12. This sample appears to be pure anatase, no other phases were observed. Similarly for sample 2 (TiCl_4 + Butanol, calcined at 450 °C) the XRD pattern reveals that the phase is pure form of anatase, the sample is highly crystalline with excellent peak intensities when titania particles were prepared using isopropanol as a solvent then calcined at 700 ° C there is a noticeable change in crystallinity of the sample.

The intensity of each of the peaks has improved but the sample shows the formation of mixture of phases as rutile and anatase. The phase of sample prepared using ethanol (95%) as solvent and calcined at 800 °C looks like rutile phase of TiO_2 . There are sharp peaks at 2θ 27.84 °, 36.44 °, 39.55 °, 41.59 °, 44.39 ° which resemble with the pure rutile phase. But along with rutile phase there are some impurities or formation of some other phase. The small peaks at 25.65°, 48.42 ° 2θ have been identified which resemble with pure phase of anatase.

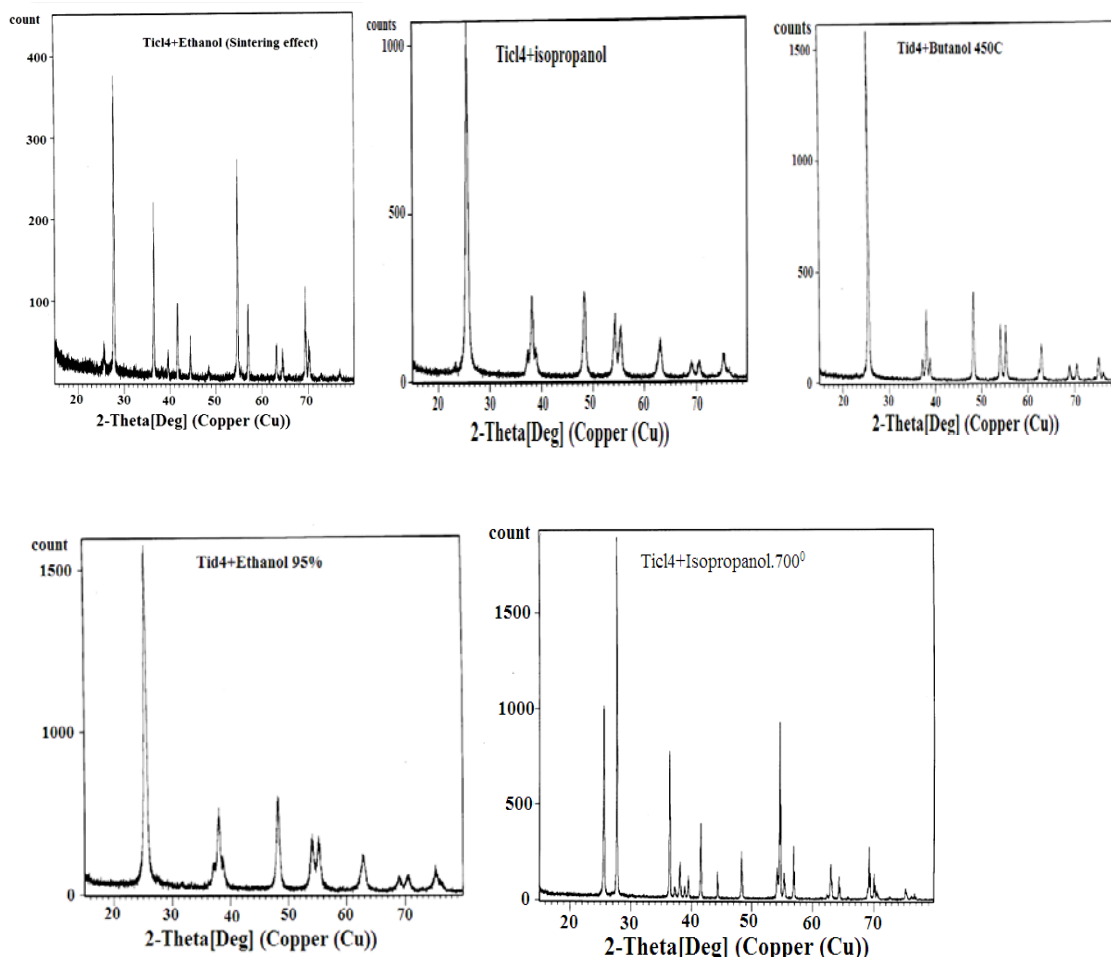


Fig 4.12 XRD pattern of sample 1 to 5

The intensity of the peaks which correspond to anatase phase is very low whereas the rutile phase intensity is quite high which indicate the formation of titania particle predominately in rutile phase. The table 4.3 summarizes the effect of solvent and temperature on the crystallite size and phase of TiO_2 synthesized by sol-gel technique.

Table 4.3 : Effect of solvent and Temperature on crystallite size and phase of TiO_2

Chemicals	Calcination Temperature	Crystalline size (nm)	Lattice parameter	Phase of TiO_2
TiCl_4 + Ethanol	450°C	22 ± 2	a=b= 3.78520 c=9.51390	Anatase
TiCl_4 + Iso-propanol	450°C	24.77 ± 2	a=b= 3.78520 c=9.51390	Anatase
TiCl_4 + Butanol	450°C	47.51 ± 2	a=b= 3.78520 c=9.51390	Anatase
TiCl_4 + Iso-propanol	700°C	2.497 ± 2	a=b= 4.59330 c=2.95920	Rutile

4.5.4 Morphology of particles

SEM images of particles of different samples also revealed that the crystallinity of the particles varied as observed by XRD analysis. Fig 4.13 shows the images of particles calcined at 450⁰ C. Samples prepared from ethanol and butanol (Fig 4.13 b and c) appear more crystalline.

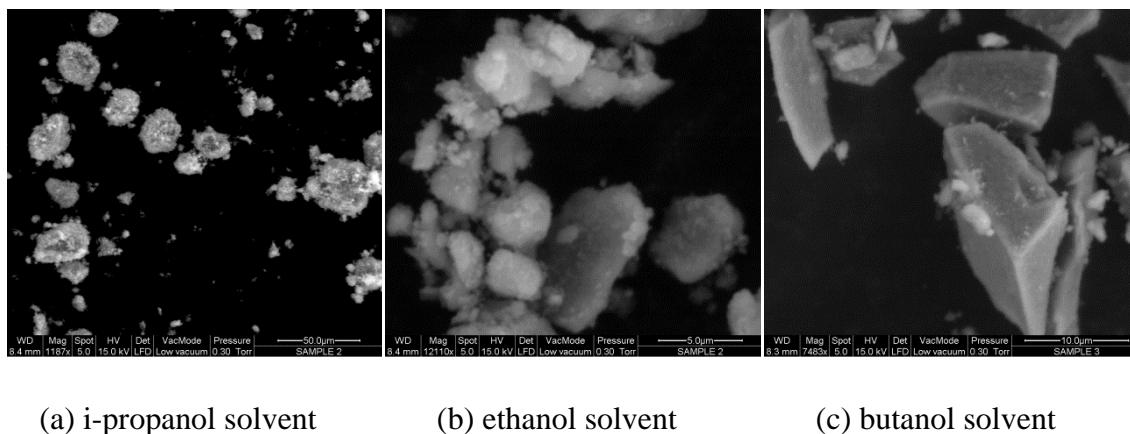


Fig. 4.13 SEM pictures of titania particles synthesized by sol-gel technique in different solvents

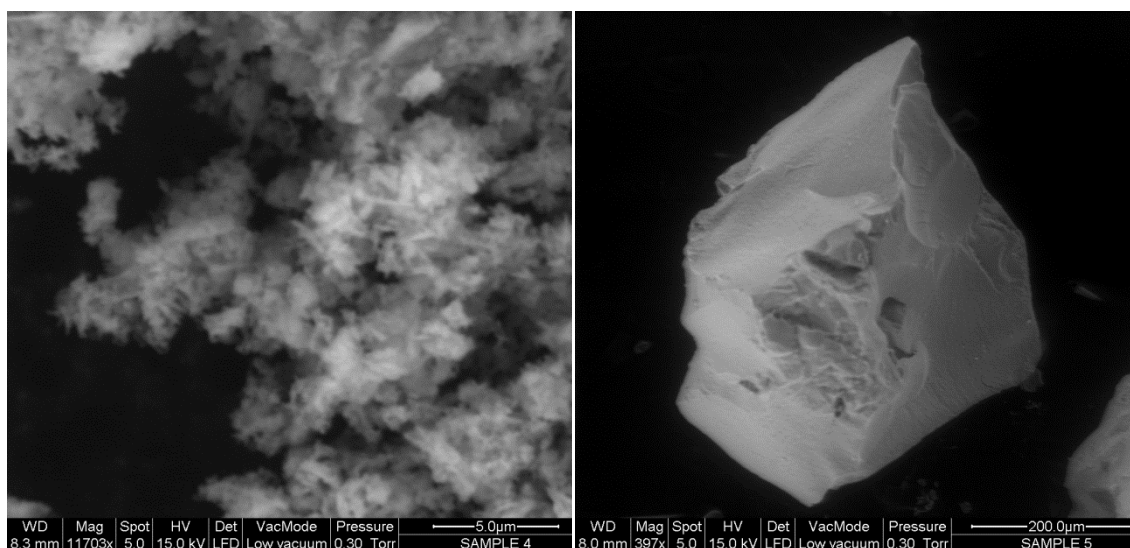


Fig 4.14 SEM images for effect of calcining temperature

4.6 Solution phase synthesis of cadmium selenide (CdSe)

Low temperature synthesis of Cadmium Selenide (CdSe) particles was performed by the *microemulsion method* and *hydrothermal method*. The CdSe particles synthesized were also characterized for their material properties, morphology and size by techniques such as X-ray diffraction, FTIR spectroscopy and Scanning electron microscopy. Further, the Photoluminescence behavior of synthesized particles was also characterized using fluorescence spectrophotometer.

4.6.1 Synthesis of CdSe in reverse micelles

Reverse micelles and Microemulsions are often used as synonymously, although there is a thin line of difference between these two phases. Usually nonionic surfactants lead to the formation of reverse micelles in organic media when there is a small presence of aqueous media in the system, the amount of water present is significantly low that satisfies the hydration of the hydrophilic head group of the surfactant. This water is not free, and its properties are different from normal water. If the amount of water present exceeds to that required for hydration of the hydrophilic head group of the amphiphile, then there will be both free and bound water in the water pool and the reverse micelle can be termed as microemulsion.

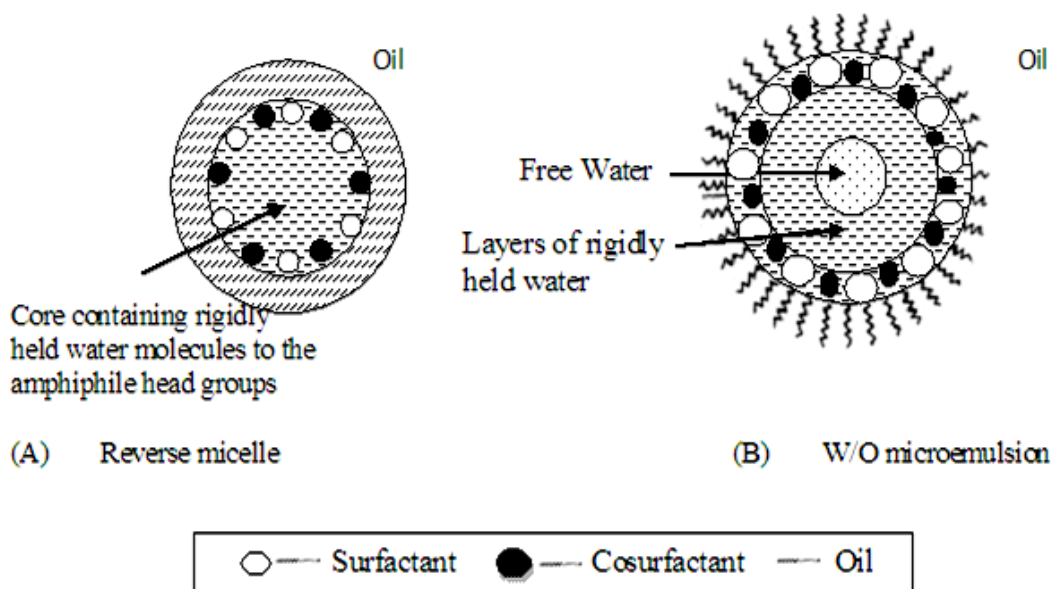


Fig 4.15 Pictorial representation of microemulsion and reverse micelles

As in the case of microemulsion synthesis of titania, the synthesis of CdSe in reverse micelles was performed as discussed in Chapter 3. Experiments were performed for base case, molar ratio (1:1) of cadmium nitrate tetra-hydrate to sodium selenite as well as for excess Cd where the molar ratio of cadmium nitrate tetra-hydrate to sodium selenite was maintained at 2:1 and also excess Se where the molar ratio of cadmium nitrate tetra-hydrate to sodium selenite was maintained at 1:2, to investigate the effect of precursor mole ratio on the CdSe particles and their respective characteristics. Table summarizes the experimental runs performed.

Table 4.4: Various experimental cases for Reverse micelle method

Sample run	Cd Salts	Se Salts	N ₂ H ₄ *H ₂ O	n-Heptane	TRITON X100
	Mmol	mmol	ml	ml	ml
Base case	2.78	2.78	5	5	10
Excess Cd case	5.56	2.78	5	5	10
Excess Se case	2.78	5.56	5	5	10

4.6.2 Characterization of the Samples:

Samples were classified by convenient notations. Characterization of particles was done using Phase analysis, XRD and SEM.

4.6.2.1 Phase Analysis

The XRD patterns of the as prepared CdSe particles along with the position of the peaks for components present in the sample are shown in Figures 4.16 to 4. 17.

It can be inferred from Figure 4.16 that most of the diffraction peaks from the CdSe particles are consistent with the wurtzite structure of CdSe with lattice constants of $a = 4.299 \text{ \AA}$ and $c = 7.010 \text{ \AA}$. There is likely possibility of formation of oxide and hydrate forms of CdSe as indicated by XRD spectra.

Figure 4.17 reveals that there is lesser degree of crystallinity when Cd precursor in excess. Matching the experimental XRD data with ICDD standard indicates that CdSe formed in this case had cubic structure. The CdSe phase in these particles was only 47.7%. The existence of wurtzite structure was not identified.

There is considerably increase in oxides - Cadmium Selenate, Cadmium Selenite, etc. that are monoclinic in nature.

Excess of Se leads to formation of particles having distinct diffraction peak of CdSe particles with 69.7% phase of CdSe of which 56.3% of Hexagonal structure and 13.4% of cubic structure as seen in Figure 4.18. There is also formation of CdSe oxides that were also formed when Cd was in excess.

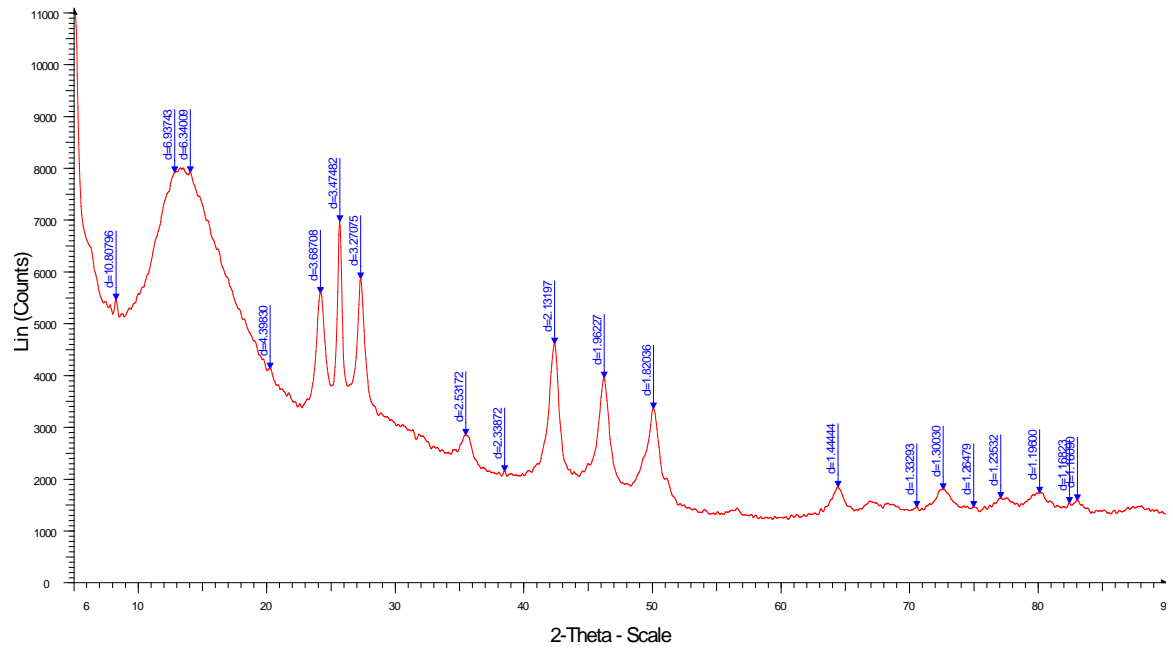


Fig 4.16 XRD patterns of the as prepared CdSe particles for base case

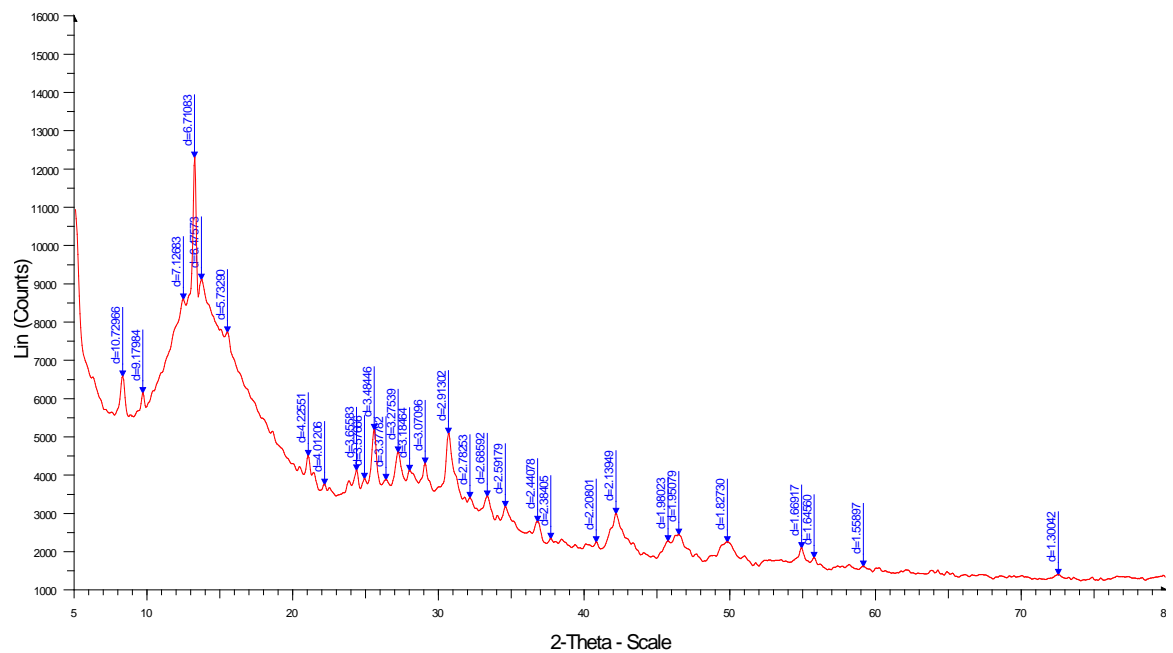


Fig 4.17 XRD patterns of the as prepared CdSe particles for excess Cd

Table 4.5 summarizes the results of XRD patterns for CdSe particles obtained using reverse micelle technique. It can be seen that CdSe phases formed varies with precursors concentration. When equimolar concentration of Cd and Se was taken, the CdSe phase was 97.7%. However, two crystalline structures were identified where hexagonal structure accounted for 66.2% while cubic structure accounted for 31.6%.

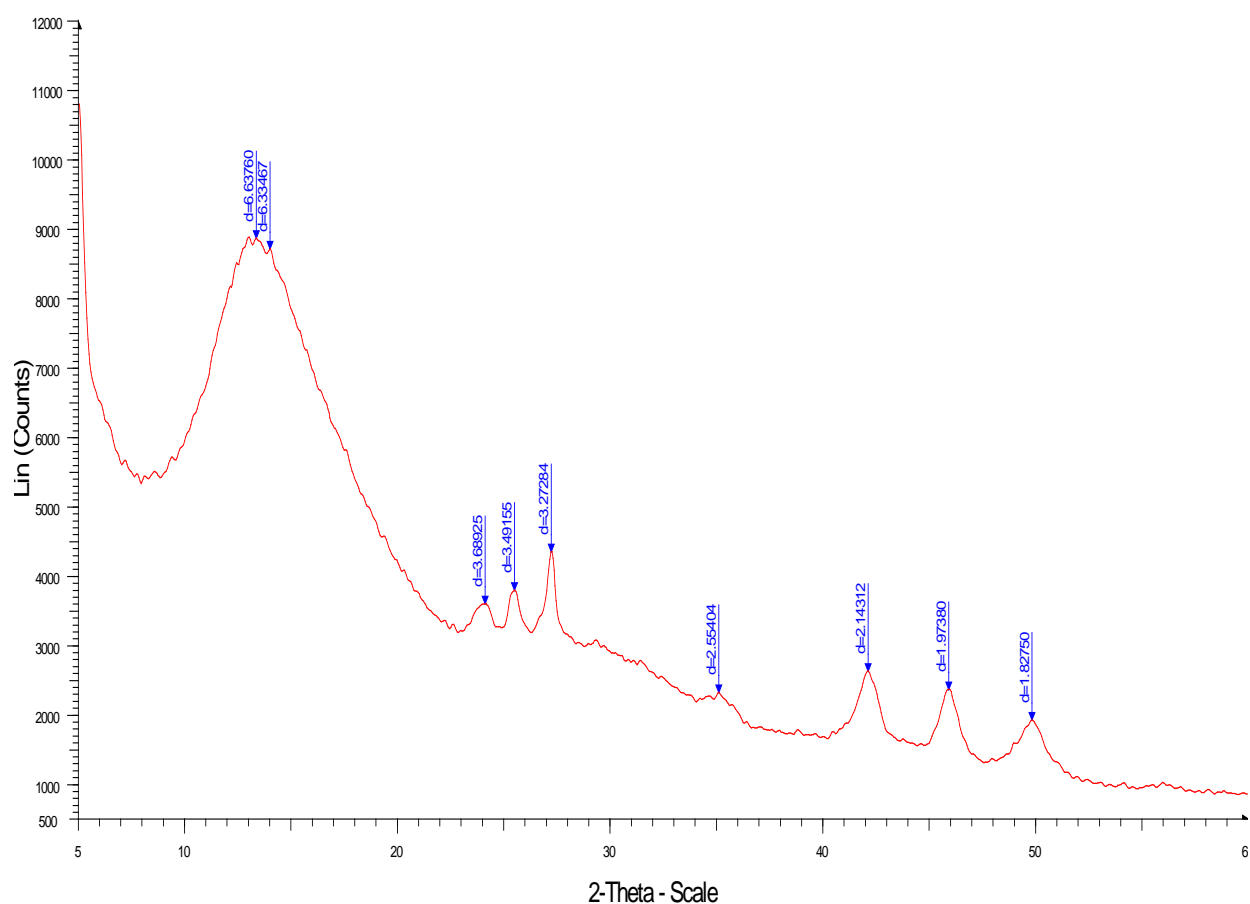


Fig 4.18: XRD patterns of the as prepared CdSe particles for excess Se

Results of phase analysis indicates that excess amount of either of the precursors is not beneficial to the synthesis of CdSe particles and therefore should be avoided when wurtzite structure (hexagonal) is desired.

Table 4.5: XRD test summary for Reverse micelle method

Sample name	Card No.	Formula	Chemical Name	%	FWHM (30)	Crystallite size	System	Cell parameter
Base case	01-070-2554 (N)	CdSe	Cadmoselit, syn	4.00	0.803°	101.3 Å	hexagonal	a = 4.2990 c = 7.0150
	00-019-0191 (I)	CdSe	Cadmium Selenide	31.60	0.297°	273.9 Å	Cubic	a = 6.077 Fixed
	00-008-0459 (I)	CdSe	Cadmoselite , syn	62.20	0.691°	117.6 Å	hexagonal	a = 4.2990 c = 7.0100
Excess Cd Salts	01-087-0513 (*)	Cd(SeO3) (H2O)	Cadmium Selenate Hydrate	2.30	0.985°	82.5 Å	Orthorhombic	a = 13.180 b = 5.8904 c = 5.056
	01-082-1165 (*)	Cd(Se2O5)	Cadmium Selenate	13.70	1°	81.4 Å	Monoclinic	a = 8.024 b = 11.319 c = 6.020 beta = 119.380
	00-019-0191 (I)	CdSe	Cadmium Selenide	47.70	0.435°	187.1 Å	Cubic	a = 6.077 Fixed
Excess Se Salts	00-051-0155 (I)	Cd(SeO3)	Cadmium Selenite	19.20	0.81°	100.4 Å	Monoclinic	a = 5.70845 b = 12.82836 c = 8.58604 beta = 101.210
	00-016-0297 (Q)	Cd3Se4O11	Cadmium Selenite	19.30	0.878°	92.7 Å	Not Available	Not Available
	00-016-0297 (Q)	Cd3Se4O11	Cadmium Selenite	30.20	0.982°	82.8 Å	Not Available	Not Available
Excess Se Salts	00-019-0191 (I)	CdSe	Cadmium Selenide	13.40	0.714°	113.9 Å	Cubic	a = 6.077 Fixed
	00-008-0459 (I)	CdSe	Cadmoselite , syn	54.50	0.553°	147.1 Å	hexagonal	a = 4.2990 c = 7.0100
	00-002-0330 (D)	CdSe	Cadmium Selenide	1.80	0.427°	190.3 Å	hexagonal	a = 4.3000 c = 7.0200

4.6.2.2 Morphology Analysis

The morphologies of the CdSe nanoparticles were characterized using Scanning electron microscopy (SEM). The morphologies of the CdSe particles were mainly affected by the Cd Salts and Se Salts precursor concentration. SEM images of CdSe particles for Base case with 20000X and 50000X are shown in Figure 4.19 and 4.20. Self similarity of these images indicates fractal growth and highly agglomerated state of the particles. Careful observation of Figure 4.20 shows dendritic growth of nanorods of CdSe having sizes significantly lower than 100 nm.

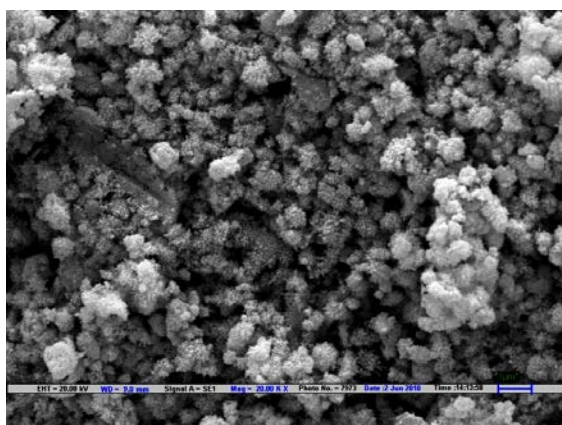


Fig 4.19 SEM image of Base case at 20000X for Reverse micelle method

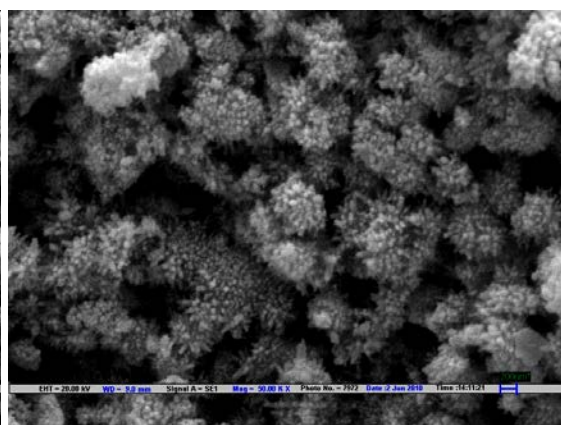


Fig 4.20 SEM image of Base case at 50000X for Reverse micelle method

SEM images of CdSe particles for Excess Cd with 50000X are shown in Figure 4.21. The extent of aggregation in these images is even more than earlier case. SEM images of CdSe particles of excess Se with 50000X are shown in Figure 4.22. In this case, the directed growth of structures forming cadmium selenite towers is observed. However, the greater morphology remains identical to the previous cases.

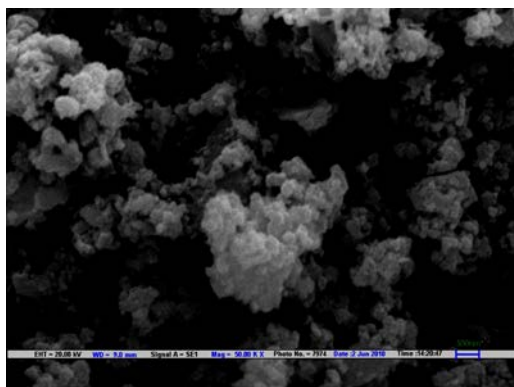


Fig 4.21 SEM image of Excess Cd (50000X)

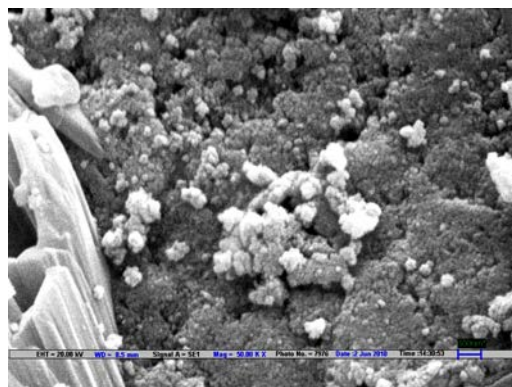


Fig 4.22 SEM image of Excess Se (50000X)

4.6.3 Hydrothermal Method

The objective of performing the hydrothermal synthesis was to identify the nature of CdSe phases formed under equimolar conditions in situations where the restriction imposed by the size of the system was eliminated. Experiments were performed for base case, molar ratio (1:1) of cadmium nitrate tetra-hydrate to sodium selenite. Experiments were also performed by varying amount of hydrazine hydrate and water (reaction media) to investigate the effect of the same on synthesis of CdSe particles and their characteristics. Table 4.6 summarizes the experimental runs performed.

Table 4.6 Summary of experimental runs performed

Sample run	Cd Salts	Se Salts	N ₂ H ₄ *H ₂ O	Deionized Water in Cd Salts	Deionized Water in Se Salts
	mmol	mmol	ml	ml	ml
RB1	2.78	2.78	10	20	20
RB2	2.78	2.78	5	20	20
B1	2.78	2.78	20	100	100
B2	2.78	2.78	10	100	100
B3	2.78	2.78	5	100	100
B4	2.78	2.78	0.42	100	100

It can be seen from Fig 4.23 and Table 4.7 that CdSe phases formed varies with amount of hydrazine hydrate, and amount of water as reaction media. From Figs. 4.23 to 4.24, it can be inferred that most of the diffraction peaks from the CdSe particles are consistent with the cubic structure of CdSe with lattice constants of $a = 6.077$ °A. However, there is also existence of CdSe with hexagonal structure with lattice parameters of $a = 4.299$ °A and $c = 7.010$ °A. There is likely possibility of formation of oxide and hydrate forms of CdSe as indicated by XRD spectra.

Fig 4.24 reveals that there is lesser degree of crystallinity when we have 20 ml (maximum amount) of hydrazine hydrate (stripping agent) and maximum of water, the reaction media. Matching the experimental XRD data with ICDD standard indicates that CdSe formed in this case had cubic structure. The CdSe phase in these particles was only 64.7%. The existence of wurtzite structure was not identified.

There is considerably increase in oxides - Cadmium Selenate, Cadmium Selenite, etc. that are monoclinic in nature.

Fig. 4.23 reveals that there is even lesser degree of crystallinity for case of 0.42 ml (minimum amount) of hydrazine hydrate and maximum of water. Matching the experimental XRD data with ICDD standard indicates that the existence of wurtzite structure or cubic structure was not identified. There are only oxides - cadmium selenate, cadmium selenite, etc. phases present that are monoclinic in nature. Dilution of the stripping agent leads to different pathways for the precipitation to proceed not resulting in the formation of CdSe.

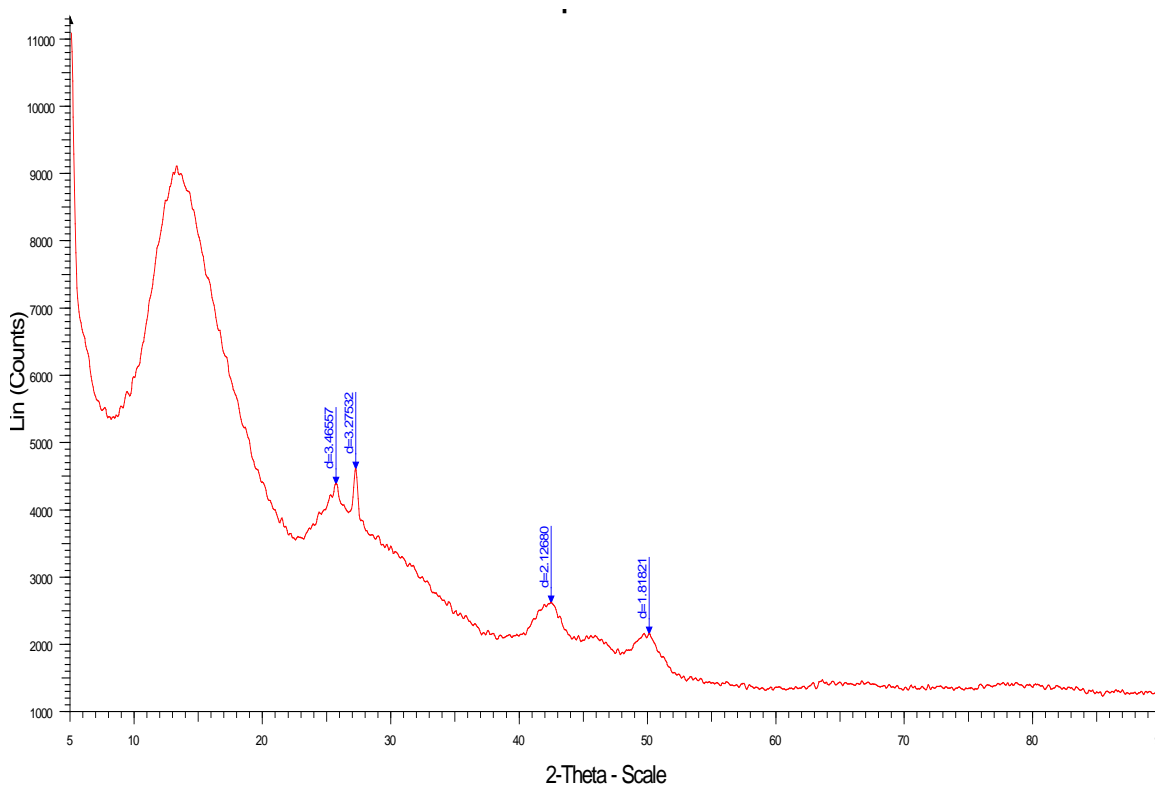


Fig 4.23 XRD pattern of as-prepared CdSe particles for B1 case

Figs. 4.23 and 4.24 reveals that there is better degree of crystallinity for case of equi-molar Cd:Se ratio with reduced amount of water content and variation of amount of hydrazine hydrate. Matching the experimental XRD data with ICDD standard indicates that CdSe formed in this case had cubic structure. The CdSe phase in these particles was only 36.8% for 10 ml hydrazine hydrate case and 27.8% for 5 ml hydrazine hydrate case. The existence of wurtzite structure was identified only in

10 ml hydrazine hydrate case with 4.1% phase. There is considerably increase in oxides - Cadmium Selenate etc. that are monoclinic in nature and 29.7% of cadmium oxide formed with cubic structure.

Results indicate lower amount of water as reaction media have impact on CdSe phases further hydrazine hydrate amount has important bearing on the structure of CdSe particles. Lowering the hydrazine hydrate leads to less generation of Se^{2-} ions which could be reason for formation of oxides and hydrates of CdSe particles.

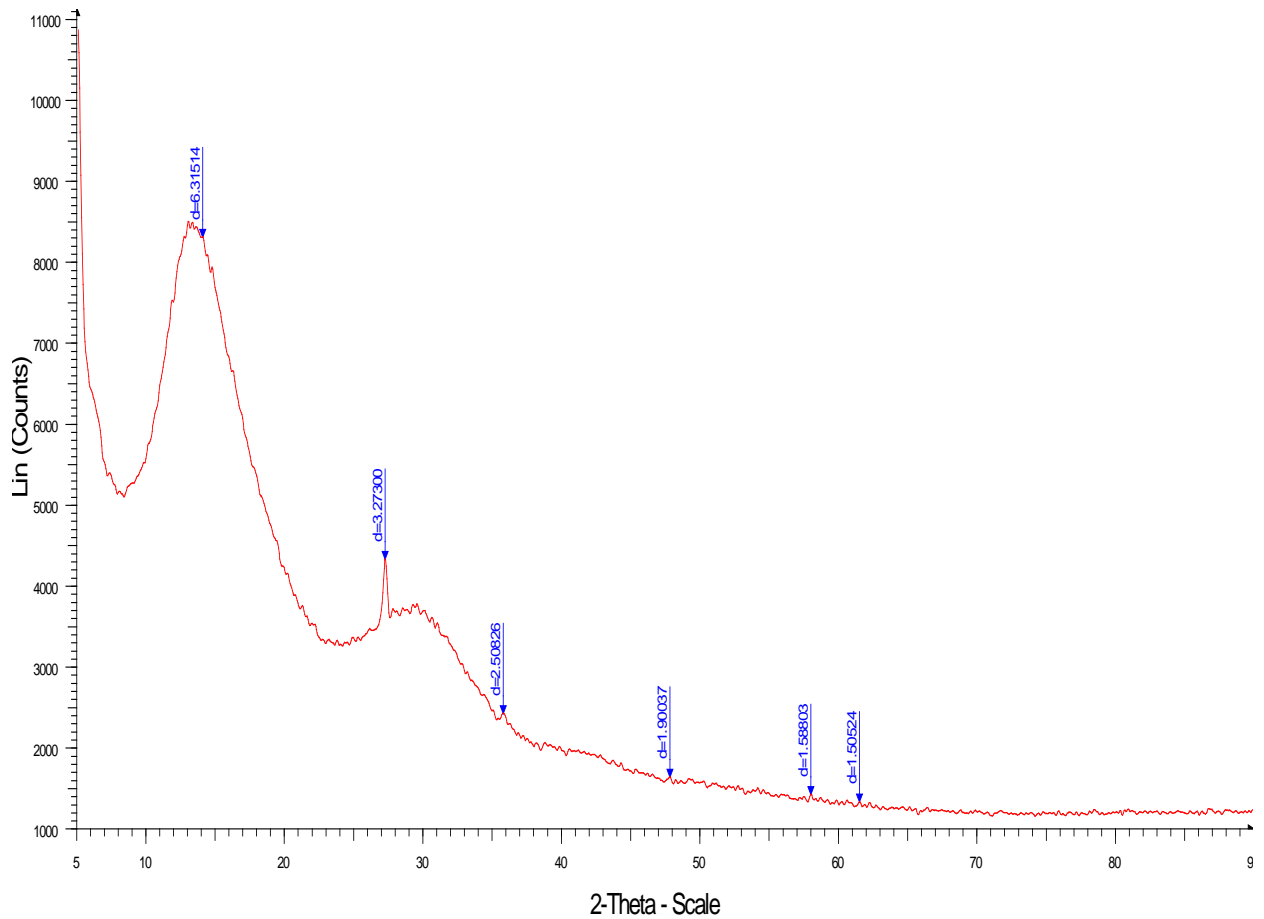


Fig 4.24 XRD pattern of as-prepared CdSe particles for B4 case

Table 4.7: XRD test summary for Hydrothermal method

Sample name	Card No.	Formula	Chemical Name	%	FWHM (3 θ)	Crystallite size	System	Cell parameter
B1	00-016-0297 (Q)	Cd ₃ Se ₄ O ₁₁	Cadmium Selenite	24.50	0.971°	83.8 °A	Not Available	Not Available
	00-002-0330 (D)	CdSe	Cadmium Selenide	3.70	0.819°	99.3 °A	hexagonal	a = 4.3000 c = 7.0200
	00-019-0191 (I)	CdSe	Cadmium Selenide	64.70	0.866°	93.9 °A	Cubic	a = 6.077 Fixed
B4	01-082-1165 (*)	Cd(Se ₂ O ₅)	Cadmium Selenate	7.00	0.859°	94.7 °A	Monoclinic	a = 8.024 b = 11.319 c = 6.020 beta = 119.380
	00-016-0297 (Q)	Cd ₃ Se ₄ O ₁₁	Cadmium Selenite	80.70	0.993°	81.9 °A	Not Available	Not Available
	01-082-1165 (*)	Cd(Se ₂ O ₅)	Cadmium Selenate	19.30	0.832°	97.7 °A	Monoclinic	a = 8.024 b = 11.319 c = 6.020 beta = 119.380
RB1	00-002-0330 (D)	CdSe	Cadmium Selenide	4.10	0.705°	115.4 °A	hexagonal	a = 4.3000 c = 7.0200
	00-019-0191 (I)	CdSe	Cadmium Selenide	36.80	0.986°	82.5 °A	Cubic	a = 6.077 Fixed
	00-002-1102 (D)	CdO	Cadmium Oxide	29.70	0.906°	89.8 °A	Cubic	a = 4.6896 Fixed
RB2	00-052-0047 (*)	CdSeO ₃ * H ₂ O	Cadmium Selenite Hydrate	9.20	0.562°	144.8 °A	Orthorhombic	a = 13.180 b = 5.890 c = 5.056
	00-051-0155 (I)	Cd(SeO ₃)	Cadmium Selenite	20.30	0.832°	97.8 °A	Monoclinic	a = 5.70845 b = 12.82836 c = 8.58604 beta = 101.210
	01-082-1165 (*)	Cd(Se ₂ O ₅)	Cadmium Selenate	72.20	0.961°	84.7 °A	Monoclinic	a = 8.024 b = 11.319 c = 6.020 beta = 119.380
	00-019-0191 (I)	CdSe	Cadmium Selenide	27.80	0.334°	243.5 °A	Cubic	a = 6.077 Fixed

4.6.3.1 Morphology Analysis

The morphologies of the CdSe nanoparticles were characterized using Scanning electron microscopy (SEM). The morphologies of the CdSe particles were affected by the amount of reducing agent Hydrazine hydrate and amount of reaction media water. SEM images of CdSe particles for RB1 case with 20000X, 50000X and 70000X are shown in Figs. 4.23, 4.24, and 4.25. Self similarity of these images indicates fractal growth and highly agglomerated state of the particles. Careful observation of Figure 4.27 shows dendritic growth of nanorods of CdSe having sizes significantly lower than 100 nm.

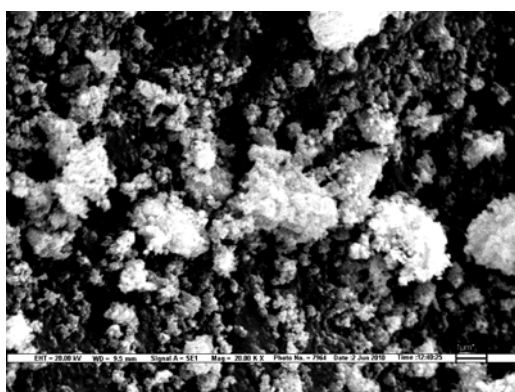


Fig 4.25 SEM image of RB1 case at 20000X for Hydrothermal method

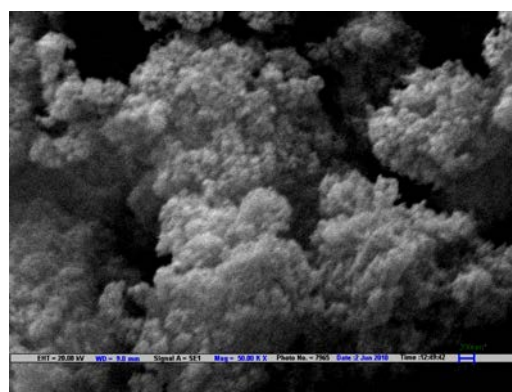


Fig 4.26 SEM image of RB1 case at 50000X for Hydrothermal method

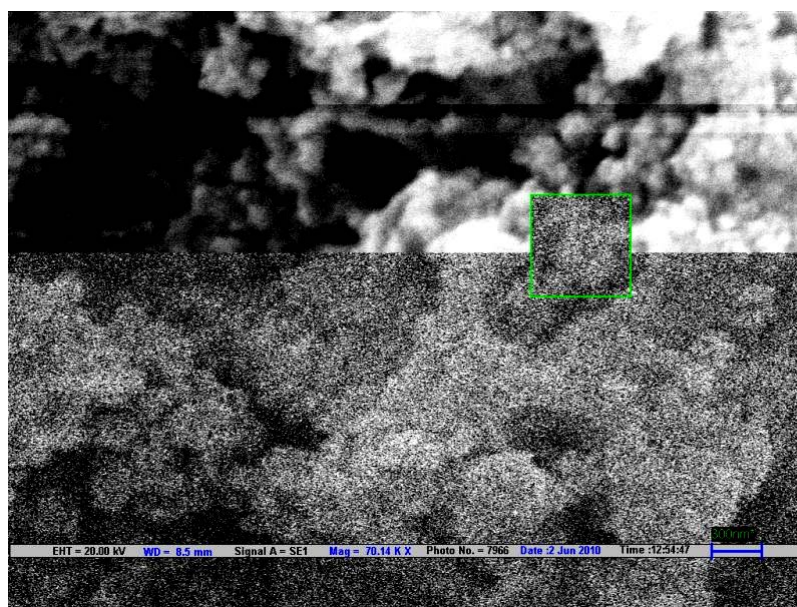


Fig 4.27 SEM image of RB1 case at 70000X for Hydrothermal method

4.6.4 Photoluminescence Spectra Analysis

In an attempt to observe the photoluminescence properties of individual CdSe particles, photoluminescence measurements were carried out on the samples using an excitation wavelength of 400 nm. The resulting PL spectra of the CdSe particles are shown in Figs. 4.28 to 4.31. The average peak in the Emission PL spectra is centred around 250 nm. The average peak in the Excitation PL spectra is centred around 400 nm. There is deviation of these peaks with the PL peak from bulk wurtzite CdSe. This may be due to oxides and hydrates forms of CdSe particles present in the reaction system. However, the sharp peak of PL spectra in the cases inferred about the existence of semiconductor particles.

The effect of precursor concentration, amount of reducing agent, and amount of reaction media can be analysed based on highest peak in PL spectra. The Emission width of peak for all three cases is almost same between 350 nm and 450nm for both techniques.

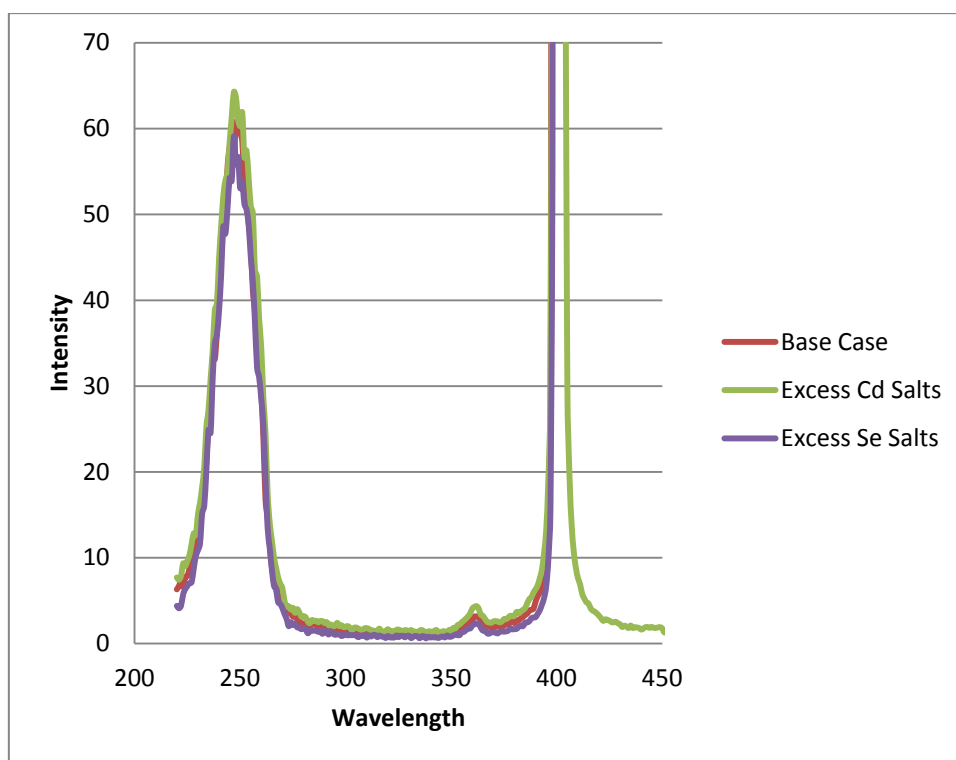


Fig 4.28 Excitation Spectra for Reverse micelle method

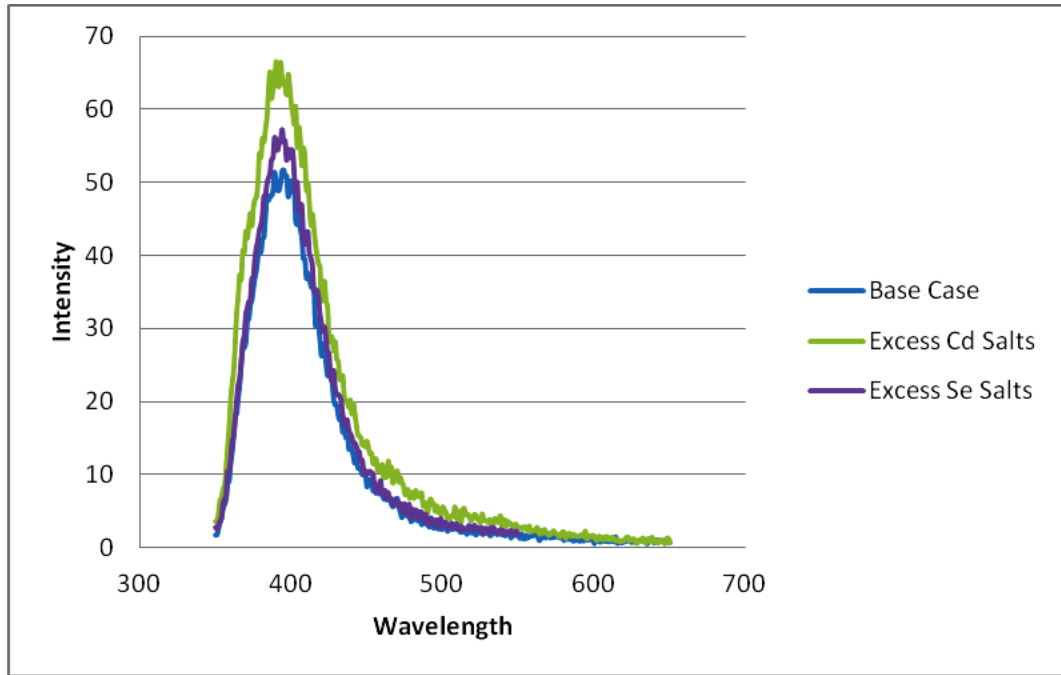


Fig 4.29 Emission Spectra for Reverse micelle method

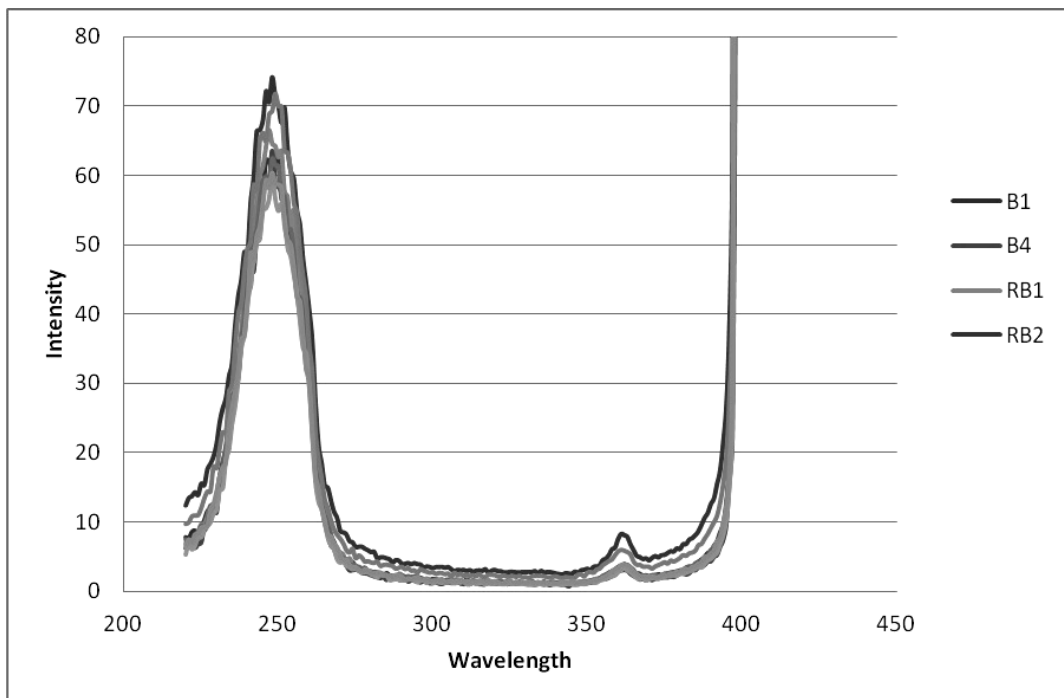


Fig 4.30 Excitation Spectra for Hydrothermal method

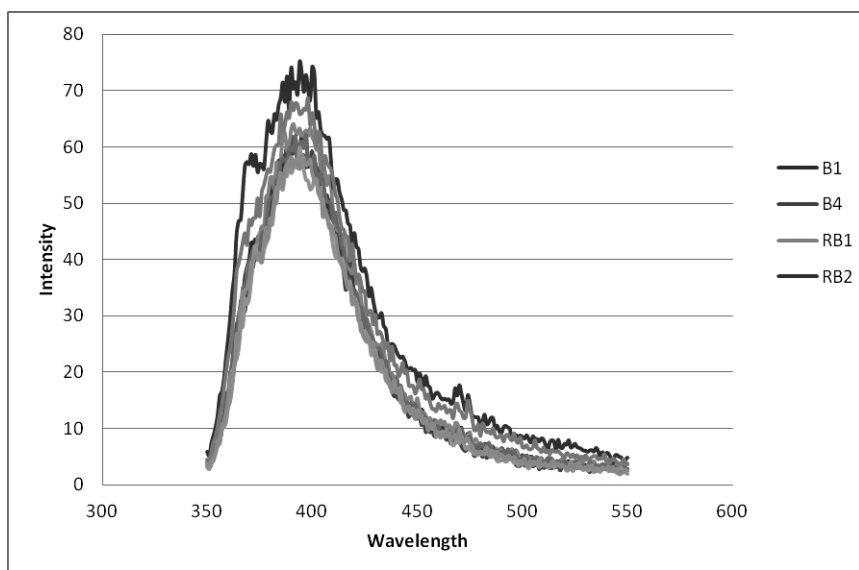


Fig 4.31 Emission Spectra for Hydrothermal method

4.7 Conclusions:

The synthesis of titania and cadmium selenide in microheterogeneous media was attempted. The results obtained are chronicled in this chapter. Pure rutile phase of titania as well as mixed phases of rutile and anatase titanium dioxide were obtained under different sets of conditions. In case of cadmium selenide synthesis mixed phases were obtained with different degree of crystallinity.

It was found that only the precipitates that were calcined for more than two hours at 800°C gave the rutile form of titanium dioxide. This in turn means that rutile titanium dioxide cannot be obtained directly using the microemulsion technique. In that case no advantage is derived from the synthesis of the material in such restricted space. The sol-gel technique also yields similar results but has the advantage that much larger amount of precipitates could be obtained. Since calcinations is necessary to obtain the titanium dioxide, it would result in change in morphology of the material and certainly leads to agglomeration of particles.

Many questions arise from this investigation that goes unanswered. What would be the most appropriate way to synthesize nanoparticles if post processing treatment like calcinations is a must? When should one opt for microemulsion methods? It is in future investigations that these questions should be attempted to be answered since these answers would establish the efficacy of this field of nanoparticle synthesis.